SCIREA Journal of Physics
ISSN: 2706-8862
http://www.scirea.org/journal/Physics
June 27, 2020
Volume 5, Issue 2, April 2020

Compositions and electrical conductivity of Al plasma: a comparison of six ionization potential depression models

W. L. Quan[1,*], Z. J. Fu[2], Y. J. Gu[3]

[1] School of Physics and Telecommunication Engineering, Yulin Normal University, Yulin 537000, China

[2] School of Electrical and Electronic Engineering, Chongqing University of Arts and Sciences, Chongqing 402160, China

[3]National Key Laboratory of Shock Wave and Detonation Physics, Institute of Fluid Physics, CAEP, Mianyang 621900, China

*Corresponding author, weilongq@126.com (W. L. Quan)

Abstract:

Recent experiments respectively performed at Linac Coherent Light Source and at Orion Laser evoke much attention on ionization potential depression (IPD) in dense plasma. In this paper, the validity of six IPD models in the warm dense region is examined, including the ion-sphere (IS) model, the Debye-Hückel (DH) model and the model proposed by Stewart and Pyatt (SP), by Ebeling (EB), and by Zaghloul (ZA), via the calculation of the compositions and electrical conductivity of dense Al plasma in a wide range of density. The big difference among these models is found at intermediate densities and low temperature. In this region, the electrical conductivities obtained with EK and ZA model are found in good agreement experiments, while those obtained with SP model are some lower and those with IS and EB

model are some higher. It suggests that EK and ZA model are more reasonable than others, since IS and EB model overestimate the IPD in warm dense region, while SP model underestimated it in this region. Nevertheless, all these models exhibit similar behaviors in low density limit, while in high density limit the DH model overestimates ionization potential depression and the rest five models are consistent with IS model.

PACS number(s): 52.25.Fi, 52.25.Jm, 52.27.Gr

Keywords: Aluminum plasma, compositions, electrical conductivity,Ionization potential depression

1 Introduction

In dense plasma, each ion/atom is exposed to the micro-field produced by free electrons and other particles; the micro-field lowers the binding energy of electrons in ions/atoms relative to the isolated ones. This phenomenon is known as ionization potential depression (IPD). The IPD shifts the equilibrium of ionization to higher charge state, which further influences the equation of state, the transport properties, and the opacity of plasma. These properties are fundamental importance in understanding the evolution of astrophysical objects, controlled nuclear fusion and other applied technologies such as plasma cutting and welding.

Since the pioneered work by Rompe and Steenbeck [1], a lot of attempts have been made to determine IPD quantitatively. In low plasma density and high temperature limit, the Debye-Hückel (DH) theory is sufficient [2, 3], while at high density the average ion-sphere (IS) model and its modifications are more favorable [4-6]. Many other extended models [7-11] have also been proposed for simulating plasma in wide range of temperature and density and some of them have been widely used in dense plasma research, *i.e.*, the Stewart and Pyatt (SP) model [8] has been adopted in many famous codes, such as LASNEX-DCA [12], CRETIN [13], FLYCHK [14], and ABAKO [15]. However, the accuracy of these models should be systematically evaluated. For example, a set of experiments [16-17] recently accomplished at Linac Coherent Light Source indicated that the K_α fluorescence spectra of dense Al plasma could not be reproduced by the SP model [8], but were consistent with the earlier model proposed by Ecker and Kröll (EK) [7]. But this opinion was not supported by the very recent

experiment independently carried out at the newly commissioned Orion Laser [18]; the spectra observed in this experiment were found to be much closer to the SP model than the EK model. This inconsistence requires more detailed investigations on the theoretical models of IPD.

On the other hand, a lot of reliable electrical conductivity data have been gained for plasma in wide density and temperature region [19-25] in the last two decades. These data are expected to be used for calibrating theoretical models. In this paper, the experimental electrical conductivity data of Al plasma are used to evaluate the validity of different IPD models. Such an evaluation is achieved as follow. First, we incorporate these IPD models into nonideal Saha equations to derive the compositions of Al plasma at varying temperature and density. Then, the obtained compositions are used to calculate the electrical conductivity of Al plasma using linear mixing rule (LMR) [26-31]. Finally, the calculated electrical conductivities are compared with the experimental data. We found that the EK and ZA model are more reasonable than other IPD models.

2 Theory and calculations

In general, the ionization equilibrium in plasma can be determined by minimizing of the Helmholtz free energy within the chemical picture. However, the free energy of dense plasma system is difficult to be calculated accurately. First, the accurate potential functions to describe the interaction among the particles are not known. Second, even if the interactions have been well represented, the configurational free energy cannot be exactly calculated since the high order virial coefficients have been neglected. Thirdly, the interactions make inner energy levels of particles in dense plasma very different from those in isolated ones, which impose additional uncertainty on the calculation of inner partition functions and then on the free energy calculations.

Considering the above approximations in free energy method, we resort to nonideal Saha equations to determine the compositions of dense plasma instead of the method of minimizing free energy. The effects of mutual interactions are taken into account by IPD models. Our calculations show that it is efficient and the obtained electrical conductivities have acceptable accuracy for Al plasma.

2.1 Nonideal Saha equations for plasma compositions

Under assumption of local thermodynamic equilibrium, compositions of dense plasma can be determined from the nonideal Saha equations,

$$\frac{n_{j+1}n_e}{n_j} = 2\frac{Q_{j+1}}{Q_j}\lambda_e^{-3}\exp\left[-\beta\left(I_j^{id} - \Delta I_j\right)\right],\quad j = 0,1,2,\cdots,z_m - 1, \tag{1}$$

where ΔI_j are the lowering of the ionization potential (LIP) of j-fold ions cause by mutual interaction, n_e is the number density of electrons, and n_j the number density, Q_j the inner partition function, and I_j^{id} the ideal ionized potential of j-fold ions. z_m is the highest charge state available in plasma. For Al plasma, we take $z_m = 13$. T is the temperature, $\beta = 1/k_BT$, and k_B is the Boltzmann constant.

Equations (1), together with conservation of nuclei

$$\sum_{j=0}^{Z_m} n_j = n_h = \frac{\rho N_A}{M}, \tag{2}$$

and conservation of charge

$$n_e = \sum_{j=0}^{Z_m} j n_j, \tag{3}$$

form a closed system of nonlinear equations to determine plasma compositions.

For given set of ΔI_j, Zaghloul showed that solution of equation system of (1)-(3) can be reduced to a simple problem of solving a single transcendental equation [32]. However, ΔI_j is not independent on compositions of plasma. It means that an iterative method has to be adopted in practical calculation for consistency. In our calculations the iterative solution of Saha equations was carried out as following: at beginning, we take $\Delta I_j = 0$ for all species and solve (1)-(3) using the method derived by Zaghloul [32] to reach a trail set of compositions. Then ΔI_j of all species are calculated from the trail compositions with IPD models. With obtained ΔI_j, Eq. (1)-(3) are resolved to give new compositions. If the new compositions are different from the old ones, recalculate ΔI_j using the new compositions and resolve Eq. (1)-(3) again until the compositions and ΔI_j satisfy the desired accuracy.

2.2 Ionization potential depression Models

Obviously, the plasma compositions calculated with nonideal Saha equations depend much on the IPD model used. In this paper, the most widely used six IPD models will be examined. They are:

A. DH model

This model is based on the Debye-Hückel (DH) theory [2, 3], in which the LIP was expressed as

$$\Delta I_j = \frac{e^2}{4\pi\varepsilon_0}\frac{(j+1)}{\lambda_D}, j = 0,1,\cdots,z_m - 1, \tag{4}$$

where λ_D is Debye radius defined by

$$\lambda_D = \sqrt{\frac{\varepsilon_0 k_B T}{e^2\left(n_e + \sum_{j=1}^{Z_m} j^2 n_j\right)}}, \tag{5}$$

with ε_0 the permittivity of vacuum and k_B the Boltzmann constant.

The DH model can well describe IPD at low densities and high temperatures, but it breaks down at high electrons densities as the Debye screen length λ_D becomes smaller than the inter-particle distance.

B. EB Model

This model was suggested by Ebeling [9] and can be taken as an improved one of the DH model. In this model, the LIP is calculated as

$$\Delta I_j = \frac{e^2}{4\pi\varepsilon_0}\frac{(j+1)}{\lambda_D + 0.125\lambda_e}, j = 0,1,\cdots,z_m - 1, \tag{6}$$

where

$$\lambda_e = \sqrt{\frac{2\pi\hbar^2}{m_e k_B T}}, \tag{7}$$

is the thermal de Broglie wavelength of electron and $\hbar$ is the reduced Plank constant, m_e is mass of electron. Comparing to the original DH model (4), it can be found that when the

density of plasma is very high, i.e., $\lambda_D << 0.125\lambda_e$, the lowering of all ions are determined by the de Broglie wavelength of electron and its dependence on density becomes very weak.

C. IS model

This is a simple approach base on the average ion-sphere (IS) model of dense plasma, where the LIP is expressed as [4]

$$\Delta I_j = \frac{e^2}{4\pi\varepsilon_0}\frac{C(j+1)}{R_j}, j = 0,1,\cdots,z_m - 1, \tag{8}$$

where $C = 1.8$ as suggested by Zimmerman and More [4]. R_j is the effective radius of a neutralized ions-sphere, defined as

$$R_j = \left(\frac{3j}{4\pi n_e}\right)^{1/3}. \tag{9}$$

By this definition, the effective ion-sphere radius of neutral atom is zero, thus, the corresponding IPD will become infinite for neutral atom. It is unreasonable and invalid for partial ionization plasma that contains neutral atoms. To extend the IS model into partial ionized plasma, we take the effective radius of neutral atom as the averaged inter-particle distance between heavy particles. That is,

$$R_0 = \bar{R}_h = \left(\frac{3}{4\pi n_h}\right)^{1/3}, \tag{10}$$

where

$$n_h = \sum_{j=0}^{Z_m} n_j, \tag{11}$$

is the number density of all heavy particles, including atoms and ions, while Eq. (9) is still adopted for ions.

D. SP model

This model was developed by Stewart and Pyatt (SP) [8]. They evaluated the micro-field surrounding an ion using the finite-temperature Thomas-Fermi model. Stewart and Pyatt derived that the LIP in plasma could be expressed as

$$\Delta I_j = \frac{e^2}{4\pi\varepsilon_0}\frac{3}{2}\frac{(j+1)}{\lambda_D}\frac{\left[1+\left(R_j/\lambda_D\right)^3\right]^{2/3}-1}{\left(R_j/\lambda_D\right)^3}, j = 0,1,\cdots z_m - 1, \tag{12}$$

where R_j has the same definition as Eq. (9) and λ_D is the Debye screening length. In high temperature limit, $\lambda_D >> R_j$, it can be found that $\Delta I_j = \frac{e^2}{4\pi\varepsilon_0}\frac{(j+1)}{\lambda_D}$, reduces to the DH model, while at high density and low temperature, where $R_j >> \lambda_D$, $\Delta I_j = \frac{e^2}{4\pi\varepsilon_0}\frac{3}{2}\frac{(j+1)}{R_j}$, which is similar to the IS model but with $C = 1.5$. This model has been adopted in many codes for simulation of plasma.

E. EK model

This model was developed by Ecker and Kröll [7]. Since the EK model can cover a wide density range below and above the so-called critical density with nondegenerate free electrons, it has also been widely used in literature. In the simplified EK model, the LIP was expressed as

$$\Delta I_j = \begin{cases} \frac{e^2}{4\pi\varepsilon_0}\frac{(j+1)}{\lambda_D}, n_e + n_h \le n_{cr} \\ \frac{e^2}{4\pi\varepsilon_0}\frac{(j+1)}{\bar{R}}, n_e + n_h \le n_{cr} \end{cases}, j = 0,1,\cdots z_m - 1, \tag{13}$$

where n_c is a critical density, defined as

$$n_c = \frac{3}{4\pi}\left(\frac{4\pi\varepsilon_0 k_B T}{z_m^2}\right)^3, \tag{14}$$

and $\bar{R}$ is the averaged inter-particle distance for all the species presented in plasma, especially, electrons are also included. That is

$$\bar{R} = \left(\frac{3}{4\pi\left(n_e + n_h\right)}\right)^{1/3}. \tag{15}$$

F. ZA model

This model was suggested by Zaghloul [10]. In this model the LIP was given by

$$\Delta I_j = \frac{e^2}{4\pi\varepsilon_0}\frac{(j+1)}{\sqrt{\lambda_D + \left(\frac{2}{3}\bar{R}\right)^2}}, j = 0,1,\cdots z_m - 1, \tag{16}$$

where λ_D is Debye screening length defined by Eq.(5) and $\bar{R}$ is defined by Eq.(15).

Comparing these IPD models with each other, it can be found that all the six models have a uniform expression as

$$\Delta I_j = \frac{e^2}{4\pi\varepsilon_0}\frac{(j+1)}{R^{eff}}, j = 0,1,\cdots z_m - 1. \tag{17}$$

It is similar to coulomb potential but with different definition of the effective radius, R^{eff}. In the DH model, the effective radius is defined as the Debye screening length, in the EB model it is a sum of the Debye screening length and thermal wave length of electron, while in the IS model it is the radius of a fictitious neutral sphere, in the EK model it is the average distance between particles and in the ZA model it is a combination of Debye length and the average distance.

2.3 Linear mixing rule (LMR) for electrical conductivity

To calculate the electrical conductivity we use linear mixture rules. Many calculations[26-31] have shown that LMR has outstanding capability for predicting the electrical conductivity of plasma with minimized computational effort and reasonably accuracy; its results are comparable to experimental measurements in a wide range of density and temperature, either fully or weakly ionized. Within LMR, the electrical conductivity of partial ionized plasma is calculated as

$$\frac{1}{\sigma} = \frac{1}{\sigma_{en}} + \frac{1}{\sigma_{ei}}, \tag{18}$$

where σ_{en} and σ_{ei} are the electrical conductivities associated with electron–atom and the electron–ion collisions, respectively. The electron-neutral conductivity is expressed as

$$\sigma_{en} = \sqrt{\frac{\pi}{8k_B T m_e}}\frac{z_{av}e^2}{\alpha_0 \bar{Q}_{en}}, \tag{19}$$

where $z_{av} = n_e / n_H$, is the average ionization state of plasma, $\alpha_0 = n_0 / n_h$ is the fraction of the neutral species. $\bar{Q}_{en}$ is the average electron-atom momentum transport cross section that

should be calculated from quantum scattering theory with the Born approximation or partial wave method. Alternatively, an analytic function derived by Desjarlais [33] is used herein for simplicity. That is

$$\bar{Q}_{en}=\left(\frac{\alpha_D}{2r_0a_B}\right)^2\frac{\pi^3}{A_\kappa^2+3B_\kappa kr_0+7.5C_\kappa\left(kr_0\right)^2+3.4D_\kappa\left(kr_0\right)^3+10.6668E_\kappa\left(kr_0\right)^4}, \tag{20}$$

with

$$\begin{aligned}
&A_\kappa=1+2\kappa r_0+\frac{7}{\pi^2}\left(\kappa r_0\right)^2+\frac{\pi}{7}\left(\kappa r_0\right)^3, B_\kappa=e^{-18\kappa r_0},\\
&C_\kappa=\frac{1+22\kappa r_0-11.3\left(\kappa r_0\right)^2+33\left(\kappa r_0\right)^4}{1+6\kappa r_0+4.7\left(\kappa r_0\right)^2+2\left(\kappa r_0\right)^4},\\
&D_\kappa=\frac{1+28\kappa r_0+13.8\left(\kappa r_0\right)^2+3.2\left(\kappa r_0\right)^3}{1+8\kappa r_0+10\left(\kappa r_0\right)^2+\left(\kappa r_0\right)^3},\\
&E_\kappa=1+0.1\kappa r_0+0.3665\left(\kappa r_0\right)^2,
\end{aligned} \tag{21}$$

and

$$r_0=\left(\frac{\alpha_D a_B}{2z_{av}^{1/3}}\right)^{1/4}, k=\frac{\left(8m_e k_B T/\pi\right)^{1/2}}{\hbar}, \kappa=1/\lambda_D, \tag{22}$$

where α_D is the polarizability of atom and for Al atom we take $\alpha_D=6.8\times10^{-24}cm^{-3}$ [34]. a_B is Bohr radius.

The electron-ion conductivity is given by Spitzer-Härm expression developed for fully ionized plasma with considering the electron-electron collisions. That is [35]

$$\sigma_{ei}=\frac{T^{1.5}}{38z_{av}}\frac{\gamma_e}{\ln\Lambda}, \tag{23}$$

where $\ln\Lambda$ is the coulomb logarithm, representing the classical collision cross section integral for electrons interaction with ions of charge z_{av}. From the classical binary cutoff theory it can be derived as [36]

$$\ln\Lambda=\frac{\pi}{2}\sin\left(x\right)\left[1-\frac{2}{\pi}\left(\mathrm{Si}\left(x\right)+\frac{\mathrm{Ci}\left(x\right)}{\tan\left(x\right)}\right)\right], \quad x=\frac{1.5}{\Lambda} \tag{24}$$

where Ci and Si are the cosine and sine integrals. The factor γ_e in Eq. (23) is a function

of z_{av}, representing the contribution arising from electron-electron scattering, written as

$$\gamma_e(z_{av}) = \frac{3\pi}{32}\left(1+\frac{153z_{av}^2+509z_{av}}{64z_{av}^2+345z_{av}+288}\right) \tag{25}$$

3 Results and discussions

3.1 Lowering of ionization potential

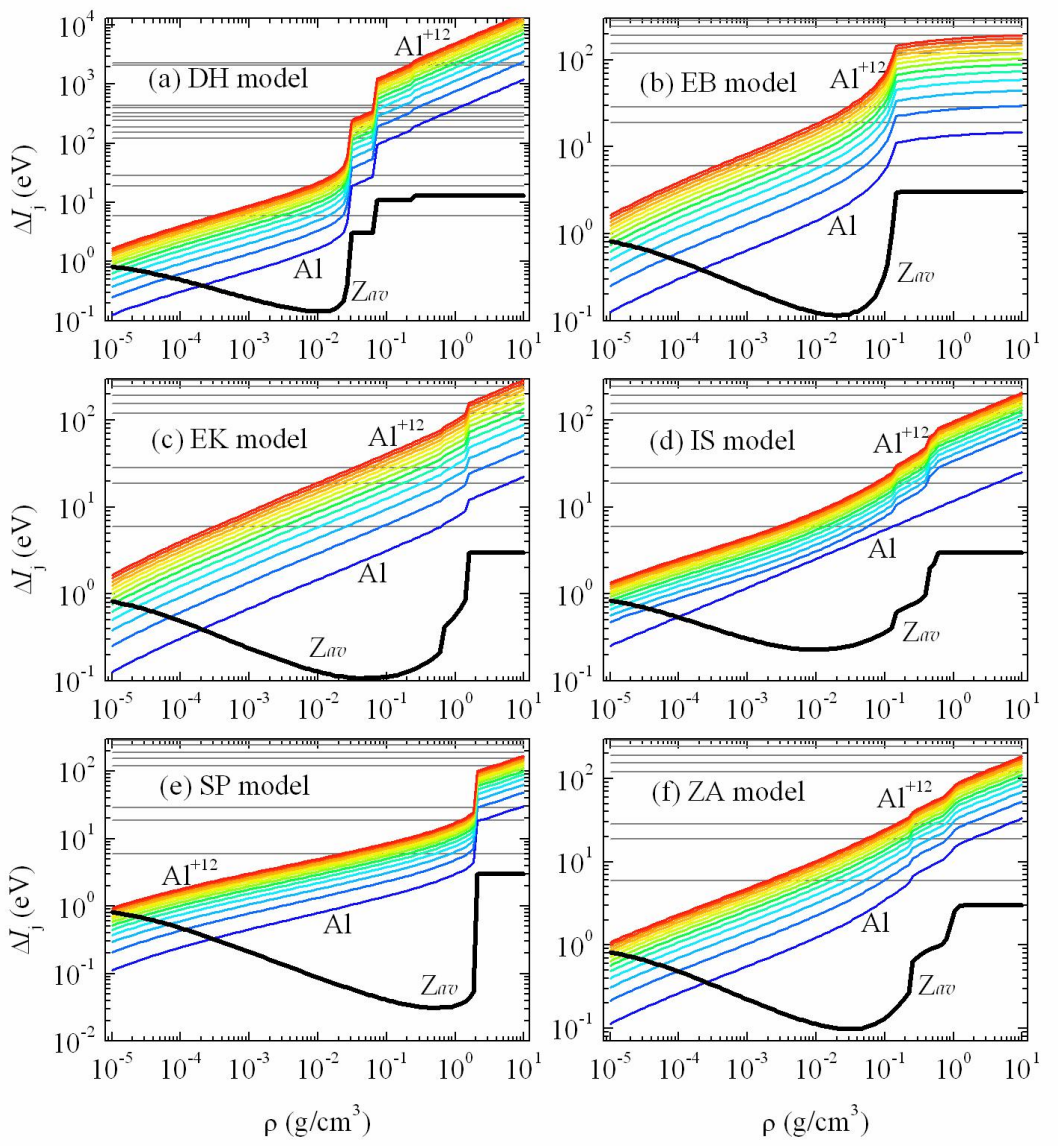

Fig.1. (Color online) Lowering of ionization potential calculated with different IPD models for Al plasma at 10^4 K. (a) DH model, (b) EB model, (c) EK model, (d) IS model, (e) SP model, (f) ZA model. From down to up, Colored lines are lowering of ionization potentials for Al, Al^{+1},…, up to Al^{+12} respectively. Horizontal gray lines are ideal ionization potentials correspondingly. Thick lines are degrees of ionization.

Fig.1 shows the density dependence of the LIPs of Al, Al^{+1}, up to Al^{+12} at 10^4 K. It can be seen that the LIPs increase with the charge of ion and density of plasma, which stands for all the six IPD models. This trend roots in the fact that all the six models describe the LIP by a formulas like $\Delta I_j \propto (j+1)/R^{eff}$, where the effective radius R^{eff} decreases with density.

It is also shown that the LIPs of all species simultaneously skip (or abruptly increase) at some densities. The LIPs skip three times for the DH model, at ~0.03, 0.07 and 0.22 g/cm^3, one times for the EB model, at ~0.15 g/cm^3, two times for the EK model, at ~0.6 and 1.6 g/cm^3, three times for the IS model, at ~0.15, 0.44 and 0.6 g/cm^3, one times for the SP model, at ~2 g/cm^3, and two times for the ZA model, at ~0.25 and 1 g/cm^3, respectively. Interestingly, all the skips of LIP are companied by an abrupt increment of ionization degree. It indicated that the skip of LIP results from the abrupt increment of electron density.

Taking the DH models as example, the first skip of LIP occurs at ~0.03 g/cm^3, at which the degree ionization abruptly increases from 0.1 to 3. Comparing the LIPs to the corresponding ideal ionization potential, it can be found that at 0.03 g/cm^3 the LIPs of Al, Al^+, Al^{+2} and Al^{+3} become larger than the corresponding ideal ionization potential while the LIP of Al^{+4} does not. It means that the effective ionization potentials of Al, Al^+, Al^{+2} and Al^{+3} become negative at 0.03 g/cm^3, while that of Al^{+4} is still positive. Such a case is maintained up to 0.07 g/cm^3. As a results, the degree of ionization steady at 3 until density reaches 0.07 g/cm^3. From 0.07 to 0.22 g/cm^3, the LIPs of ions up to Al^{+10} become larger than their ideal ionization potential, but the LIP of Al^{+11} is still lower than its ideal ionization potential, which make the degree of ionization steady at 11. For higher density, the LIPs of Al^{+11} and Al^{+12} also become higher than their ideal ionization potential, thus, the ionization degree is finally steady at 13.

Similar analysis can be taken out for the rest five IPD models. However, for these models the highest degree of ionization that can be reached is only 3 at high density, since the LIPs of Al^{+4} and higher charge states calculated with these five models are never higher than the corresponding ideal ionization potential, while the LIPs of Al, Al^+, Al^{+2} and Al^{+3} are larger than the corresponding ideal ionization potentials at high density.

Another observation should be noted is that at high densities (>2 g/cm^3), the LIPs given by the DH model are about thousands of eVs, while those of other models are only about hundreds of eVs at the same densities. The very high LIP of the DH model at high density is incorrect since the hypostasis of the DH model cannot be fulfilled at high density.

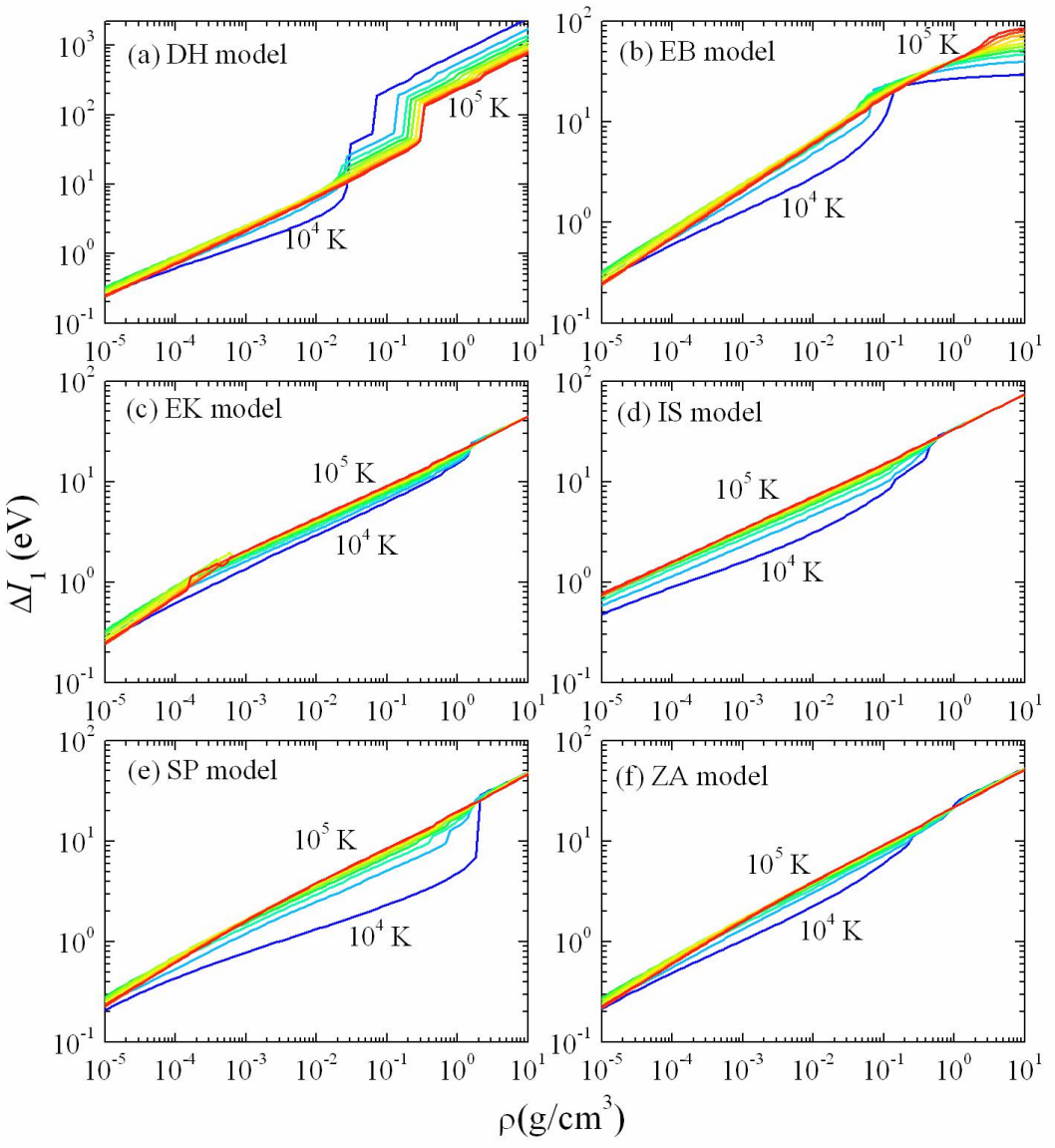

Fig.2. (Color online) Influence of temperature on the lowering of ionization potential of Al^{+1} calculated with different IPD models. Lines from black to green are corresponding to the temperature from 10^4 K to 10^5 K with interval of 10^4 K.

To illustrate the temperature dependence of these IPD models, the LIP of Al^{+1} at different plasma temperature (from 10^4 to 10^5 K with interval of 10^4 K) is shown in Fig.2. For all the six models, the LIPs increase with temperature at low densities, while at high density the LIP decreases with temperature except the EB model. However, at high densities the decrement of LIP caused by temperature is very small for the EK, IS, SP and ZA model, but for DH model, the decrement of LIP is remarkable, while in the case of the EB model, the LIP increases with temperature since thermal wave length is used in this model.

3.2 Composition of Al plasma

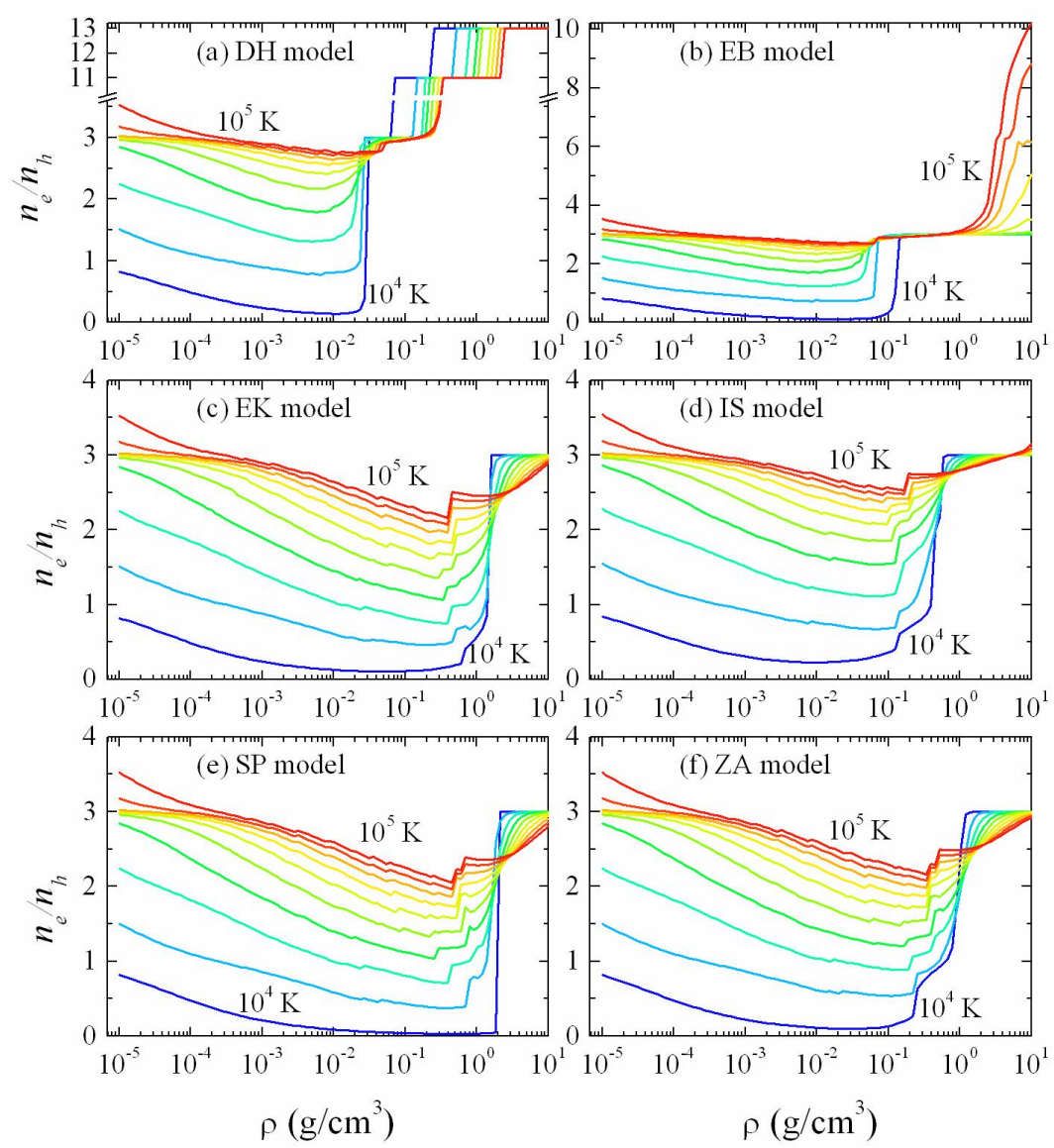

Fig.3. (Color online) Degree of ionization calculated with different IPD models for Al plasma in the whole range of temperature and density considered. Lines from black to green are corresponding to the temperature from 10^4 K to 10^5 K with interval of 10^4 K.

Now we can discuss the compositions of Al plasma predicted by these models. Fig.3 shows the degrees of ionization of Al plasma at different temperatures as function of density. It can be seen that at given temperature the degree of ionization decrease slightly and then abruptly increase with density, which stands for all six models. It indicates that all the six models can well reflect the pressure induced ionization.

As far as the effect of temperature is concerned, it can be seen that the degree of ionization

increases with temperature at low densities, which is tenable for all the models. However, at high densities, the degree of ionization decreases with temperature for the DH, EK, IS, SP, and ZA models, while for the EB model, it increases with temperature. Another effect is that as the temperature increases, the critical density of pressure induced ionization, namely, the density at which the degree of ionization abruptly increases, shifts to higher density for DH model, but for other models it shifts to lower density.

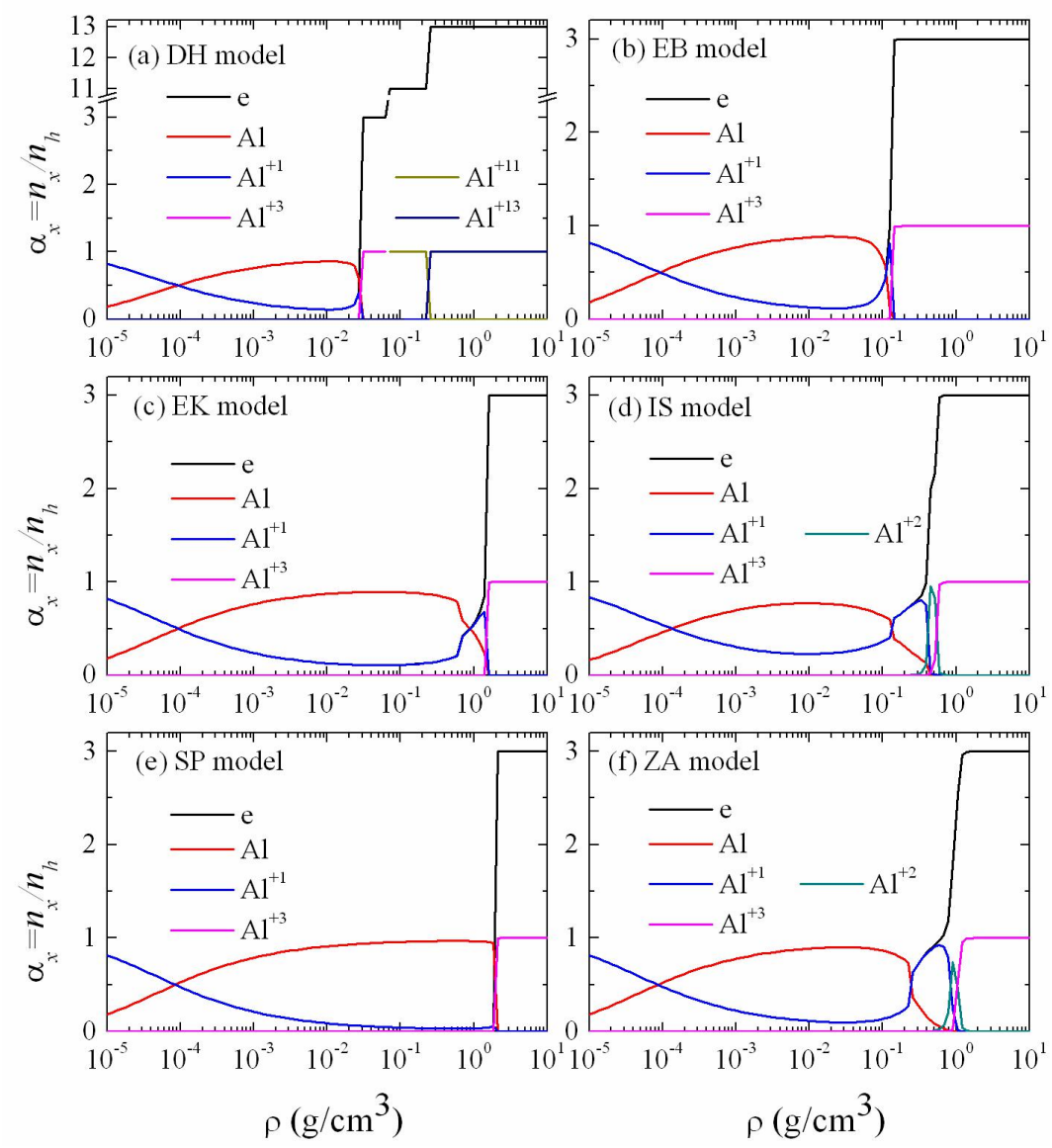

Fig.4. (Color online) Compositions of Al plasma at 10^4 K are shown as a function of density.

Fig.4. shows the compositions of Al plasma at 10^4 K as an example. It shows that for all six models, the density range considered can be divided into two segments. In low density range, Al plasma is partial ionized plasma and is mainly constituted by Al, Al^{+1} and electrons; the

fraction of Al atoms firstly increases and then quickly decreases with density, while the fraction of Al^{+1} firstly decreases and then increases with density, standing for all six models. In high density range, plasma is fully ionized. However, the EB, EK, IS, SP and ZA model predict that the Al plasma is constituted by Al^{+3} and electrons, while the DH model predicts that it is constituted by Al^{+11} and electrons from 0.07 to 0.15 g/cm^3 and by Al^{+13} and electrons for higher density. For IS and ZA model, Al^{+2} also present at transition density.

The above trends in the degree of ionization and compositions can be explained as following: at low density range, the plasma is dominated by the thermal ionization since the LIPs given by these models are relative small compared to the corresponding ideal ionization potentials. In this region, the Saha equation (1) reduces to $\left(\frac{n_e}{n_0}\right)^2 = \frac{1}{n_0} 2 \frac{Q_1}{Q_0} \lambda_e^{-3} \exp\left[-\beta\left(I_0^{id} - \Delta I_0\right)\right]$, Clearly, the degree of ionization decreases with density and increases with temperature. At high density range, the increase of degree of ionization with density is caused by the pressure induced ionization. it make the LIPs of Al, Al^+, Al^{+2} and Al^{+3} given by these models (except the DH model that can not be used at high density) larger than the corresponding ideal ionization potentials. That is, at high density the pressure induced ionization makes the Al^{+3} become more stable than others. As a result, increasing temperature lead to decrease of degree of ionization since the combination of electrons and ions becomes easier.

3.3 Electrical conductivity of Al plasma

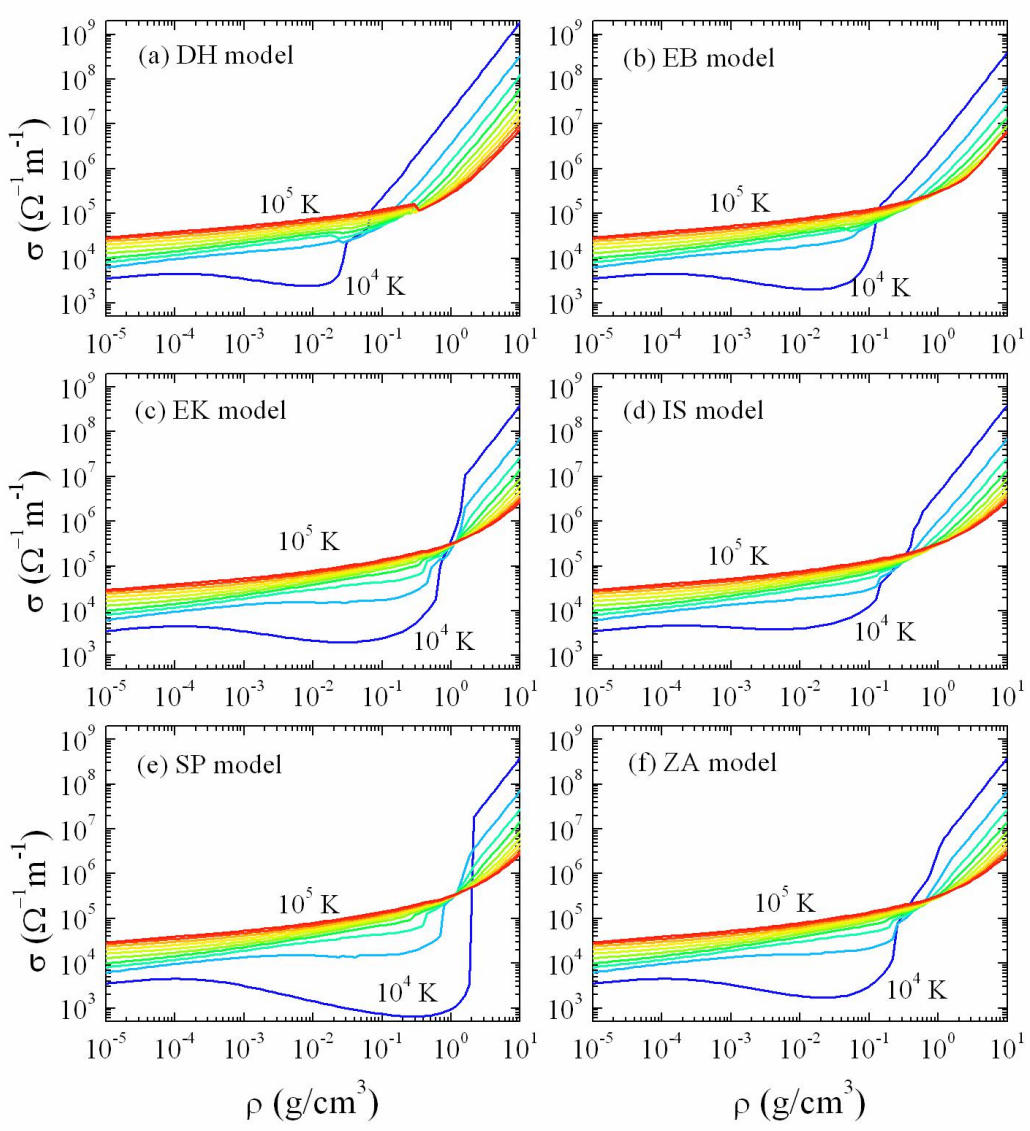

Fig.5. (Color online) Electrical conductivities calculated with different IPD models for Al plasma in the whole range of temperature and density. In each panel, lines from black to green are corresponding to the temperature from 10^4 K to 10^5 K with interval of 10^4 K.

Based on the obtained compositions, we further calculate the electrical conductivities of Al plasma with linear mixing rule. The results are plotted as a function of density in Fig.5.

At relative low temperature (i.e., 10^4 K, black line), the dependence of electrical conductivity on density can be divided into three characteristic regions: (i) A low density region where the electrical conductivity increases with density; (ii) an intermediate density region where the electrical conductivity slightly decreases with density; and (iii) a high density region where the conductivity abruptly increases with density. As the plasma temperature increases, the electrical conductivities in both of region (i) and (ii) increase with temperature, and in region (ii) the increments caused by temperature are larger than in region (i), whereas in region (iii)

the electrical conductivity decreases with temperature.

As having been shown in Fig.4, at 10^4 K, the Al plasma is mainly constituted by Al, Al^{+1} and electrons, the higher ionized state can be neglected in region (i). In this region, the LIPs of Al and Al^{+1} are always lower than their ideal ionization potential (Fig.1), thus the effective ionization potential of them are positive. According to Saha equations, the electron density increases with temperature and density in region (i). At the same time, the momentum transfer cross section of electrons-ions/atoms scattering is almost independent on temperature because the interaction is very weak in this region. As a result, in region (i) the conductivity increases with temperature and density, which is main caused by the increase of the electron density. In region (ii), the electrical conductivity increase of with temperature and decreases with density, this can be attributed to the variation of ionization degree, which increases with temperature and decreases with density. In region (iii), the electrical conductivity increase with density is cause by the increment of electron density, while its decrement of with temperature results from the increase of the momentum transfer cross section and decrease of the degree of ionization with temperature.

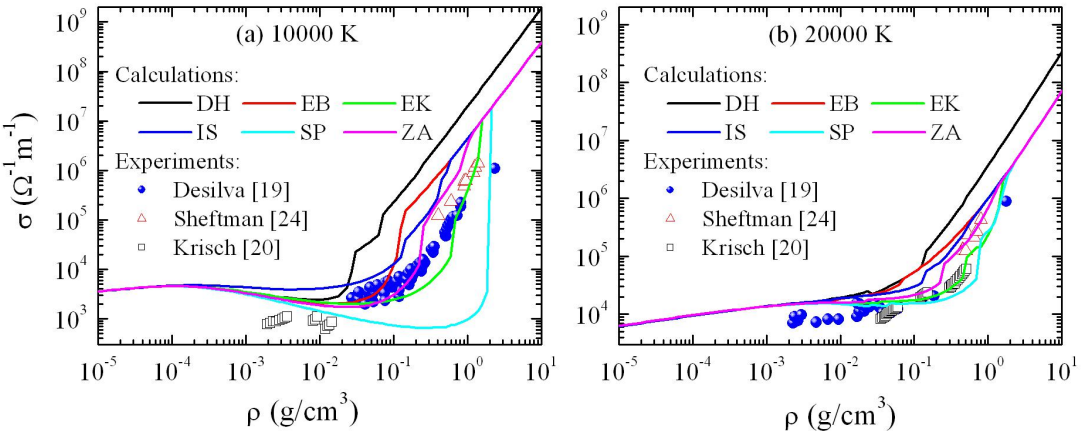

Fig.6. Comparison of calculated electrical conductivity of Al plasma with available experimental data.

In Fig.6, electrical conductivities of Al plasma at 10000 and 20000 K are compared with experimental measurements by Desilva [19], Krisch [20] and Shelftman [24]. For the case of 10000 K, the electrical conductivity calculated by the EK and ZA models are the closest to experiments, whereas that from the model SP is much smaller, and those from the DH, EB and IS are obviously larger than experiments. However, all six models have identical low density limit that can be well described by the Debye-Hückel theory. At high density, the results with the EB, EK, SP, ZA are almost identical to that with the IS model, but the result

with the DH model is some high. As temperature increases to 20000 K, the difference in the electrical conductivity calculated by these models becomes small. The results of the DH model are still higher than experiments, while the results of other five models are in good agreements with experiments. Even so, the results of the EK and ZA models are closer to experiments than other models.

4 Summary

The compositions of Al plasma are calculated with nondieal Saha equations in which the effect of interactions is taken into account by six different models of ionization potential depression. To evaluate the applicability of these models the electrical conductivity of Al plasma are calculated in wide range of temperature and density with linear mixing rule and the results are compared with experimental data. Our calculation shows that:

First, at low density limit, all six models have similar behavior that is consistent with the DH theory. Second, at high density limit the EB, EK, SP and ZA have similar behavior that is consistent to the ion-sphere model, but the DH model is not. The LIPs given by the DH model are about thousands eVs at high densities and the corresponding ionization degree is 13 even the temperature is only 10^4 K; both of them are too high and unreasonable. Third, the big differences among these models are found at intermediate density, and the lower temperature, the bigger is difference. Fourth, the EK and ZA model are more reasonable than other models and SP model underestimates the LIP at low temperature. Finally, the combination of the nonideal Saha equation with linear mixing rule is a powerful routine to predict the electrical conductivity of dense plasma. Along this routine, the electrical conductivity of dense plasma can be quickly calculated and with acceptable accuracy if an appropriate model of ionization potential depression, i.e., the model suggested by Zaghloul, is adopted.

Acknowledgments

This research was financial supported by the National Natural Science Foundation of China (Grant No. 51365027), the Natural Science Foundation of Gansu province (Grant No. 18JR3RA112) and the Guangxi Natural Science Foundation (Grant No. 2019JJA110043)

References

[1] R. Rompe and M. Steenbeck, Ergeb. Exakt. Naturw. 18, 257 (1929).

[2] H. R. Griem, Phys. Rev. 128, 997 (1962).

[3] H. R. Griem, Plasma spectroscopy (McGraw-Hill Book Co., New York, 1964).

[4] G. B. Zimmerman and R. M. More, J. Quant. Spectrosc. Radiat. Transfer 23, 517 (1980).

[5] B. J. B. Crowley, Phys. Rev. A 41, 2176 (1990).

[6] J. Stein, D. Salzmann, Phys. Rev. A 45, 3943 (1992).

[7] G. Ecker, W. Kröll, Phys. Fluids 8, 62 (1963).

[8] J. C. Stewart, K. D. Pyatt Jr, Astrophys. J. 144, 1203 (1966).

[9] W. Ebeling, W. D. Kremp, and D. Kraft, Theory of Bound States and Ionization Equilibrium in Plasma and Solid (Akademie-Verlag, Berlin, 1976)

[10] M. R. Zaghloul, Phys. Plasma 15, 042705 (2008).

[11] S. I. Anisimov, Yu. V. Petrov, Teck. Phys. Lett. 23, 472 (1997).

[12] Y. T. Lee, J. Quant. Spectrosc. Radiat. Transfer 38,131 (1987).

[13] H. A. Scott, J. Quant. Spectrosc. Radiat. Transfer 71,689 (2001).

[14] H.-K. Chung, M. H. Chen, W. L. Morgan, Y. Ralchenko, R. W. Lee, High Energy Density Phys. 1, 3 (2005).

[15] R. Florido, R. Rodríguez, J. M. Gil, J. G. Rubiano, P. Martel, E. Mínguez, and R. C. Mancini, Phys. Rev. E 80, 056402 (2009).

[16] S. M. Vinko, O. Ciricosta, B. I. Cho, K. Engelhorn, H.-K. Chung, C. R. D. Brown, T. Burian, J. Chalupský, R. W. Falcone, C. Graves, V. Hájková, A. Higginbotham, L. Juha, J. Krzywinski, H. J. Lee, M. Messerschmidt, C. D. Murphy, Y. Ping, A. Scherz, W. Schlotter, S. Toleikis, J. J. Turner, L. Vysin, T. Wang, B.Wu, U. Zastrau, D. Zhu, R. W. Lee, P. A. Heimann, B. Nagler and J. S. Wark, Nature (Lond.) 482, 59 (2012).

[17] O. Ciricosta, S. M. Vinko, H.-K. Chung, B.-I. Cho, C. R. D. Brown, T. Burian, J. Chalupský, K. Engelhorn, R. W. Falcone, C. Graves, V. Hájková, A. Higginbotham, L. Juha, J. Krzywinski, H. J. Lee, M. Messerschmidt, C. D. Murphy, Y. Ping, D. S. Rackstraw, A. Scherz, W. Schlotter, S. Toleikis, J. J. Turner, L. Vysin, T. Wang, B. Wu, U. Zastrau, D. Zhu, R. W. Lee, P. Heimann, B. Nagler, and J. S. Wark, Phys. Rev. Lett.

109, 065002 (2012).

[18] D. J. Hoarty, P. Allan, S. F. James, C. R. D. Brown, L. M. R. Hobbs, M. P. Hill, J. W. O. Harris, J. Morton, M. G. Brookes, R. Shepherd, J. Dunn, H. Chen, E. Von Marley, P. Beiersdorfer, H. K. Chung, R. W. Lee, G. Brown, and J. Emig, Phys. Rev. Lett. 110, 265003 (2013)].

[19] A. W. DeSilva, J. D. Katsouros, Phys. Rev. E 57, 5945 (1998).

[20] I. Krisch and H. J Kunze, Phys. Rev. E 58, 6557 (1998).

[21] J. F. Benage, W. R. Shanahan, M. S. Murillo, Phys. Rev. Lett. 83, 2953 (1999).

[22] J. Haun, H. J Kunze, S. Kosse, M. Schlanges, R. Redmer, Phys. Rev. E 65, 46407 (2002).

[23] C. Blancard P. Renaudin, G. Faussurier, and P. Noiret, Phys. Rev. Lett. 88, 215001 (2002).

[24] D. Sheftman and Ya. E. Krasik, Phys of Plasmas 18, 092704 (2011).

[25] A.W. DeSilva, A.D. Rakhel, Contrib. Plasma Phys. 45, 236 (2005).

[26] S. C. Lin, E. L. Resler, and A. Kantrowitz, J. Appl. Phys. 26 ,40(1955).

[27] D.-K. Kim, I. Kim, Phys. Rev. E 68, 056410 (2003).

[28] D.-K. Kim, I. Kim, Contrib. Plasma Phys. 47, 173 (2007).

[29] Z. J. Fu, Q. F. Chen, X. R. Chen, X. W. Sun and W. L. Quan, Phys. Scr. 85, 045502 (2012).

[30] Z. J. Fu, Q. F. Chen and X. R. Chen, Contrib. Plasma Phys. 52, 251 (2012).

[31] Z. J. Fu, L. J. Jia, X. W. Sun, Q. F. Chen, High Energy Density Phys.9 ,258 (2013).

[32] M. R. Zaghloul, J. Phys. D: Appl. Phys. 33, 977-984 (2000).

[33] M. Desjarlais, Contrib. Plasma Phys. 41267 (2001).

[34] P. Milani, I. Moullet, W. A. de Heer, Phys. Rev. A, 42, 5150 (1990).

[35] L. Spitzer, R. Härm, Phys. Rev. 89, 977 (1953).

[36] M. R. Zaghloul, M. A. Bourham, J. M. Doster, J. D. Powell, Phys. Lett. A 262, 86 (1999).